

Article

Killing Bacteria Using Acetic Acid and Nanosecond Pulsed Electric Fields—An In Vivo Superficial Infection Model Study and Immune Response

Emilija Perminaitė¹, Auksė Zinkevičienė¹, Veronika Malyško-Ptašinskė¹ , Eivina Radzevičiūtė^{1,2} ,
Jurij Novickij², Irutė Girkontaitė¹  and Vitalij Novickij^{1,2,*} 

¹ Department of Immunology, State Research Institute Centre for Innovative Medicine, 08409 Vilnius, Lithuania

² Faculty of Electronics, Vilnius Gediminas Technical University, 10223 Vilnius, Lithuania

* Correspondence: vitalij.novickij@vilniustech.lt

Abstract: Invasive infections caused by drug-resistant bacteria are a problem responsible for many fatal cases, especially in burn wound care centers, while bacterial resistance to antibiotics is growing dramatically worldwide. In this work, we utilize pulsed electric fields (up to 25 kV/cm × 750 ns) in combination with low-concentration (1%) acetic acid for the inactivation of *P. aeruginosa*. An in vivo superficial infection model is developed in BALB/C mice using a luminescent strain of *P. aeruginosa*. We show that an up to 25 kV/cm electric field (3 kV, 1.2 mm gap), when combined with acetic acid, induces a bacteriostatic effect, preventing further infection for up to 7 days after treatment. Additionally, we evaluate antibodies against surface and intracellular *P. aeruginosa* bacteria antigens following the treatment. It is shown that the levels of surface IgG and IgG1 antibodies are significantly lower in the murine serum of electric-field-treated mice compared to the bacterial-infection-bearing group of mice treated with acetic acid alone. The results of this work are useful as a proof of concept for the development of novel clinical procedures to fight drug-resistive microorganisms responsible for wound contamination and chronic wounds.

Keywords: acetic acid; bacteria; electroporation; *P. aeruginosa*; skin infection



Citation: Perminaitė, E.; Zinkevičienė, A.; Malyško-Ptašinskė, V.; Radzevičiūtė, E.; Novickij, J.; Girkontaitė, I.; Novickij, V. Killing Bacteria Using Acetic Acid and Nanosecond Pulsed Electric Fields—An In Vivo Superficial Infection Model Study and Immune Response. *Appl. Sci.* **2023**, *13*, 836. <https://doi.org/10.3390/app13020836>

Academic Editor: Gyungsoon Park

Received: 18 November 2022

Revised: 4 January 2023

Accepted: 6 January 2023

Published: 7 January 2023



Copyright: © 2023 by the authors. Licensee MDPI, Basel, Switzerland. This article is an open access article distributed under the terms and conditions of the Creative Commons Attribution (CC BY) license (<https://creativecommons.org/licenses/by/4.0/>).

1. Introduction

In recent years, the constant development of wound management techniques and dressings to overcome chronic wounds and enable the effective treatment of wounds associated with hospital infections or burn wounds has been observed [1–3]. The trend is shown in Figure 1. Such a demand for research is due to the increasing bacterial resistance to antibiotics worldwide, due to several contributing factors, including inappropriate antibiotic utilization in clinics and widespread use in the food industry [4]. Drug-resistant bacteria and the associated infections result in high morbidity and mortality rates [5,6]. *P. aeruginosa* is one of the leading causes of hospital-acquired infections, which also justifies the increase in scientific papers each year focusing on the multi-drug resistance of this microorganism (Figure 1). Recent studies indicate an increasing variety of virulence factors (especially toxins) in *P. aeruginosa* that is becoming a major concern for clinicians, while *P. aeruginosa* has a higher chance of infecting immunocompromised hosts [7,8]. One of the solutions is to perform preventive procedures for the control of infections with multidrug-resistant microorganisms, e.g., removal of sinks in intensive care units, better processing of waste water, etc. [9]. However, such solutions do not solve the problem completely, but reduce the number of incidents. Therefore, the interest in the development of effective methods and approaches to treat bacterial infections is high and the topic remains very relevant [10].

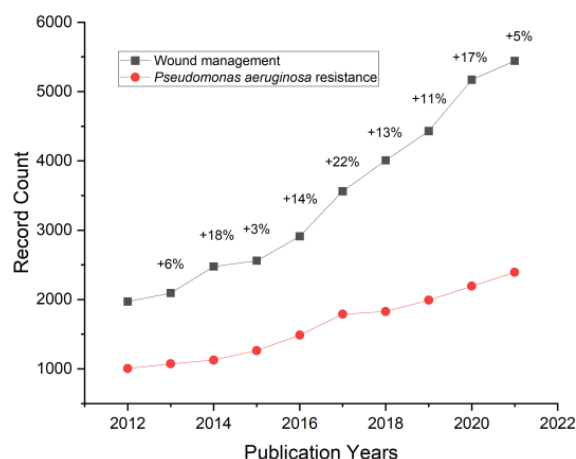


Figure 1. The trend in the number of scientific works published in the past decade on the topic of wound management. Percentages indicate the increase in the number of scientific papers each year compared to the preceding year. Visualized based on the data from Clarivate Analytics Web of Science (topic keywords: “wound management” and “*Pseudomonas aeruginosa* resistance”, access date: 13 November 2022).

The chemical antimicrobial compounds used to treat wounds are usually limited by their specific mechanism of bio-interaction, while extensive burn injuries are challenging in terms of clinical diagnosis and the rapid definition of effective antimicrobial therapy [11]. Therefore, novel techniques have to be proposed to address the multi-drug resistance of pathogenic and opportunistic microorganisms [12]. Ultimately, the approach should be universal and non-specific to a certain microorganism.

One of these approaches is the use of acetic acid (AA), which is heavily employed in hospitals to treat burn infections. The AA is applied topically within dressings and is well tolerated by patients in small concentrations; however, with higher concentrations (e.g., 5%), patients complain of stinging and pain on application of acetic acid to wounds [13,14]. Nevertheless, it does not encourage the evolution of multiple drug-resistant strains of microorganisms in hospital environments; therefore, this method remains relevant for thousands of years [15].

Another solution is to use physical methods such as photodynamic therapy or cold plasma treatment. In the case of photodynamic therapy, frequently, an additional photosensitizer has to be employed [16]. The direct exposure to plasma terminates the infection by destroying the biofilm over it; therefore, it is considered a good treatment option for wound healing [17]. The potential of pulsed electric fields (PEF) in this context has been also highlighted recently [18–20].

Subjecting cells to high-intensity PEF results in a phenomenon known as electroporation [21]. The cells are polarized in an electric field, and when a certain threshold transmembrane potential is reached, hydrophilic pores are formed in the membrane, enabling effective mass transfer [22]. If the intensity is further increased (amplitude, number of pulses or duration), the process becomes irreversible and the cells die (i.e., irreversible electroporation). This phenomenon is heavily used and is not limited to food processing as a non-thermal sterilization method [23]. In vitro data suggest the promising combination of PEF with antimicrobials, enabling the sensitization of microorganisms to chemical treatment [24–27]. Recently, our group has presented a proof of concept regarding the application of PEF with AA, which results in the effective killing of bacteria on the skin surface [5]. Nevertheless, it should be noted that a real contaminated wound is more difficult to treat, since the bacteria colonize deeper layers of the skin. Moreover, the efficiency of the method and the inflammation over time is still poorly covered in the literature. In 2021, Wu et al. showed that an antimicrobial effect can be triggered when the burn wound is treated by PEF; however, as a limitation, a skin fold between the electrodes is required to deliver

the pulses, which is not always possible in a wound treatment context [28]. The lack of precise measurements and evaluations of the penetration depth of PEF are highlighted as the main limitations of the study.

Therefore, in this work, we developed an *in vivo* superficial *P. aeruginosa* infection model and studied the potential of PEF + AA treatment. Application of PEF with a chemotherapeutic agent is advantageous due to the synergy of both treatments, which allows the inactivation of bacteria at significantly lower PEF intensities [5,29]. Additionally, we have developed a finite element method (FEM) model to assess the penetration depth of the treatment and proposed the application of tweezers—thus, there is no longer a requirement to form a skin fold to deliver the pulses effectively. *P. aeruginosa* has been selected as a model organism, since it is the predominant species responsible for up to 80% morbidity and mortality cases worldwide in the context of wound infections [30]. Due to the ability to form biofilms and various drug-resistive patterns, it is one of the most relevant microorganisms causing serious health problems according to the World Health Organization (WHO) [6]. Additionally, we have evaluated antibodies against surface and intracellular *P. aeruginosa* bacteria antigens after the PEF + AA treatment to characterize the immune response after treatment. The results of this work are useful for the development of clinical procedures to fight drug-resistive microorganisms responsible for superficial infections.

2. Materials and Methods

2.1. Electroporation Setup and Parameters

A square-wave 3 kV, 100 ns–1 ms, high-voltage pulse power generator was used for the generation of the electric field [31]. As an applicator, tweezer electrodes (gap 1.2 mm) were used, in accordance with a previously established *in vivo* model [5]. The bacteria-infected flanks of mice (BALB/C) were treated with a pulsed electric field by iterative repositioning of the electrodes to cover the whole region of interest (~10 mm diameter circle, ~78.5 mm²). The treatment was limited to two PEF protocols: (1) 15 kV/cm × 750 ns × 1000 pulses (charging voltage 1.8 kV) and (2) 25 kV/cm × 750 ns × 1000 pulses (charging voltage 3 kV). Both were delivered with a predefined 15 kHz frequency.

A low concentration (1%) of acetic acid was used as an electrode–skin interface to ensure a synergistic treatment similar to electrochemotherapy [32]. A total of 14 ± 5 repositions of the tweezer electrodes was required to cover the whole treatment area.

2.2. Bacterial Strain

Electrotransfection of *P. aeruginosa* ATCC27853 bacterial strain was performed with the pAKlux2 plasmid (Addgene plasmid #14080), as was described previously [5]. Briefly, this plasmid contains the luxCDABE operon obtained from luciferase (luxAB) and fatty acid reductase (lux CDE) genes. Therefore, only the live bacteria are bioluminescent (Figure 2).

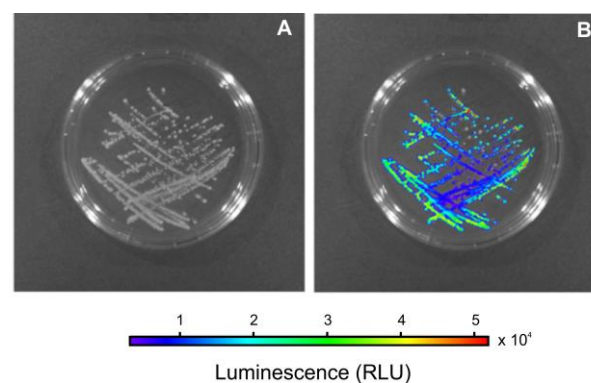


Figure 2. The black and white photo (A) and the resultant bioluminescence (B) of the successfully transformed *P. aeruginosa* strain with Addgene plasmid #14080. Acquired using IVIS Spectrum (Caliper/Perkin Elmer, Akron, OH, USA).

For experiments, bacterial cells were cultured overnight in liquid Luria–Bertani (LB) medium (10 g/L tryptone, 5 g/L yeast extract, 5 g/L NaCl) in a rotary shaker at 37 °C. Then, 1 mL of the cell culture (optical density (OD) = 1; 600 nm; 1.5×10^9 cells) was transferred to 10 mL of fresh LB medium and grown for an additional 4 h at the same conditions.

2.3. In Vivo Model

BALB/c mice were used in the experimental model ($n = 30$). The flanks of the animals were depilated using 8% $\text{Na}_2\text{S} \times \text{H}_2\text{O}$ and then washed with water. The mice were anesthetized via intraperitoneal injection of ketamine (80 mg/kg) and xylazine (10 mg/kg). A round (~10 mm diameter) area was defined for treatment, which was lightly bruised with a sharp tweezer tip to create uniform skin irritation, similar to the tape stripping technique [33]. When a homogeneous pinkish-red color of the skin surface was achieved (due to mechanical damage), the suspension of bacteria in phosphate-buffered saline (PBS) (OD = 8 at 600 nm) was transferred to the surface of the irritated skin using a pipette (50 μL) and uniformly distributed across the area. After one hour, the mice were anesthetized again following the same procedure and analyzed with the IVIS Spectrum (Caliper/Perkin Elmer, Akron, OH, USA). The animals with bacterial contamination were treated with PEF and 100 μL of 1% acetic acid was used as a skin–electrode interface.

The number of photons emitted due to bacterial bioluminescence was proportional to the live bacteria contaminating the area; therefore, all the results were normalized to the PEF-untreated control (1% acetic acid) to enable comparison among the efficacies of various treatments.

Evaluation of bacterial contamination with and without the PEF treatment was performed on days 3, 5 and 7.

The protocol was approved by the State Food and Veterinary Service (License Nr. G2-48).

2.4. Determination of Bacteria-Specific Antibodies

Antibodies (Ab) against surface and intracellular *P. aeruginosa* bacteria antigens were determined. For this assay, *P. aeruginosa* bacteria (surface Ag) and bacterial lysate (intracellular Ag) were used. The mice sera samples were obtained at day 0 and day 7. A small volume of blood (no more than 200 μL) was collected from the tail veins of the mice and the extracted serum was used for the detection of bacteria-specific antibodies. Bacterial cell suspension (prepared according to Section 2.3 and re-suspended in PBS) was treated under UV for 30 min. Bacterial lysates were prepared cells subjected to liquid nitrogen and then a 37 °C water bath; the procedure was repeated 10 times. For the determination of antibodies, 96-well plates (Nunc MaxiSorp, Thermo Fisher Scientific, Waltham, MA, USA) were used. Each well received 50 μL of the appropriate bacterial suspension or lysate (equivalent to 8×10^5 bacteria per well). The coated plate was incubated at 4 °C overnight. Each well was blocked using 150 μL of 10% fetal bovine serum (FBS) for 1 h at room temperature (RT) with shaking. The bacteria-coated wells were incubated with diluted murine serum (1:100) for 1 h at RT with shaking. Mixtures of biotin-labeled antibodies to mouse IgM (BD Pharmingen, San Jose, CA, USA), IgG1, IgG2a, IgG2b, IgG3 (BD Pharmingen) were used (1 h. RT). Then, 50 μL of streptavidin–horseradish peroxidase conjugate (BD Pharmingen) was added, followed by 30 min incubation at RT with shaking. Bound conjugate was detected colorimetrically using 100 μL of o-phenylenediamine dihydrochloride (OPD) substrate containing 0.025 M NaCOOCH_3 and 100 μL 35% H_2O_2 . The color reaction was stopped by adding 50 μL of 2 M H_2SO_4 . The plates were washed 3 times with phosphate-buffered saline with Tween (PBS-T) between each step. The optical density was read at 492 nm with a Synergy 2 microplate reader and Gen5 (v. 1.04.05) software (Biotek, Shoreline, WA, USA). The background level was subtracted from the obtained optical density values and the relative units (RU) were calculated. The antibody levels of mice after treatment (PEF + AA or AA only, $n = 8$ in each group) were normalized to the antibody levels of mice

before the treatment ($n = 6$; $RU = 100$). Controls included the following: non-coated wells, bacteria-coated wells with PBST instead of serum and wells with no conjugate.

2.5. Finite Element Method Model

The three-dimensional mouse skin model was developed in COMSOL Multiphysics, version 5.5 (COMSOL, Los Angeles, CA, USA). Due to the complexity of the skin structure and lack of availability of electrical parameters of all the skin layers, some layers were approximated as one, i.e., the dermis was combined with the epidermis and fat due to comparable electrical properties [34–36]. The stratum corneum was not introduced in the model due to light bruising, which was performed according to the procedure above (Section 2.3). A summary of the model parameters is presented in Table 1.

Table 1. Summary of the finite element model parameters.

Parameter	Value	References
Dermis conductivity	0.2–0.4 S/m; 1 S/m ^a	[34–36]
Dermis thickness	200 μ m	[37]
Muscle conductivity	0.62 S/m; 1.5 S/m ^a	[35,38]
Muscle thickness	3 mm	N/A
Electrode conductivity	1.4×10^6 S/m	[39]
Acetic acid conductivity	0.13 S/m ^b ; 0.5 S/m ^a	[40,41]
Applied voltage	3 kV	N/A
Electrode gap	1.2 mm	N/A
Skin lump height	0.25 mm	N/A

^a modeled change in conductivity due to application of electric field pulses; ^b approximated using a linear dependence; N/A—non-applicable.

One of the electrodes was selected as a ground with zero potential and the second electrode was used as a terminal (3 kV); outer boundaries were electrically insulated. Stationary analysis was performed.

The mesh and model structure are shown in Figure 3.

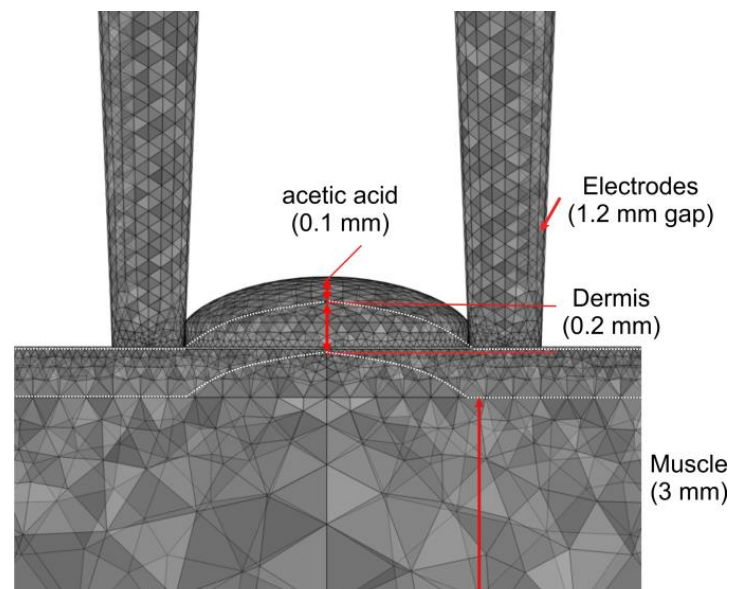


Figure 3. The mesh structure of the skin treatment using tweezer electrodes.

The mesh was formed using tetrahedral finite elements with a minimum and maximum size of elements of 36 and 496 μ m, respectively. The maximum growth rate of 1.4 was selected. The total number of elements was 1,522,135.

For Joule heating evaluation, a COMSOL embedded model of skin tissue was used (Bioheat Physics module sub-group) and a time-dependent simulation was performed.

2.6. Statistical Analysis

All the data were analyzed using GraphPad 8.0.2 Prism 6 software (GraphPad Software Inc., La Jolla, San Jose, CA, USA). A nonparametric Mann–Whitney U test was used to compare the groups of mice. Differences with a p -value < 0.05 were regarded as significant. In the graphs, the asterisk * indicates $p \leq 0.05$; ** $p \leq 0.01$; *** $p \leq 0.001$.

3. Results

Firstly, the FEM model was used to characterize the treatment and the expected PEF spatial distribution. The spatial distribution of the electric field when a 3 kV voltage was applied between the electrodes is shown in Figure 4.

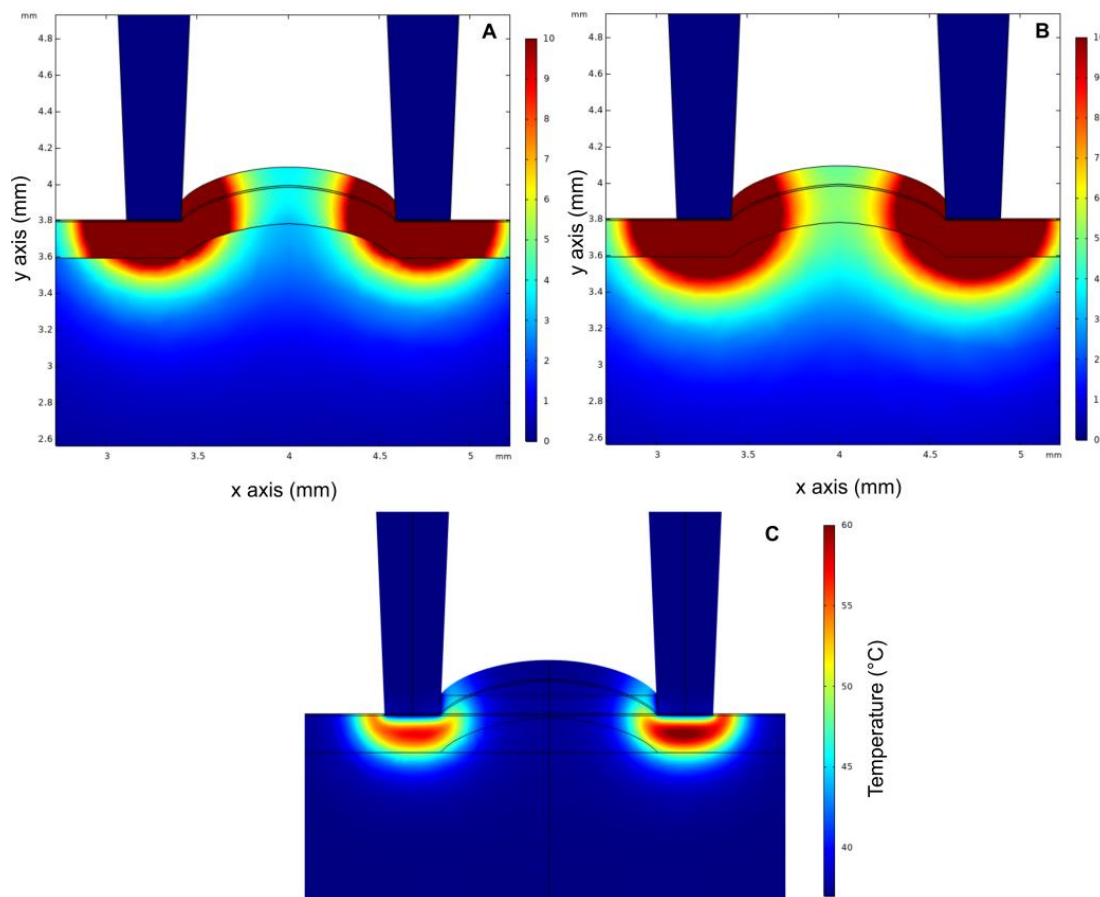


Figure 4. The spatial distribution of the electric field during pulsed electric field treatment, where (A) tissue conductivities are nominal and not affected by PEF; (B) tissue electrical conductivities are increased due to permeabilization triggered by PEF; (C) Joule heating due to PEF application. A 3 kV voltage is applied between the terminals (gap 1.2 mm). The electric field spatial distribution data are shown in kV/cm.

It can be seen that the distribution of the electric field is non-homogeneous, with the field being higher near the tips of the electrodes. In the simulation, it is assumed (and based on available knowledge) that the first few pulses in the burst trigger irreversible electroporation (Figure 4A), which results in a significant increase in the conductivity of the separate layers (refer to Table 1). As a result, the spatial distribution of PEF is altered (Figure 4B). It can be seen that the upper layers of the skin in the middle of the skin lump are subjected to PEF exceeding 6 kV/cm, while PEF up to 25 kV/cm is reached in close proximity to the electrodes. In general, the treatment is superficial, with low penetration (< 1 mm) to deeper tissue (i.e., muscle).

The Joule heating effect was analyzed after the 1000×750 ns pulse burst delivered at 15 kHz (Figure 4C). It can be seen that in close proximity to the electrodes, the temperature rises up to 61°C , which is a 24°C increase. Such an increase in temperature is in agreement with established knowledge; however, it is indicative that a further increase in the input energy is not possible.

Following the FEM analysis, the mice were treated with two nanosecond protocols ($1.8\text{ kV} \times 750\text{ ns} \times 1000$ pulses and $3\text{ kV} \times 750\text{ ns} \times 1000$ pulses) and acetic acid (1%). In both cases, the gap between tweezer electrodes was 1.2 mm. A typical response to the treatment is shown in Figure 5.

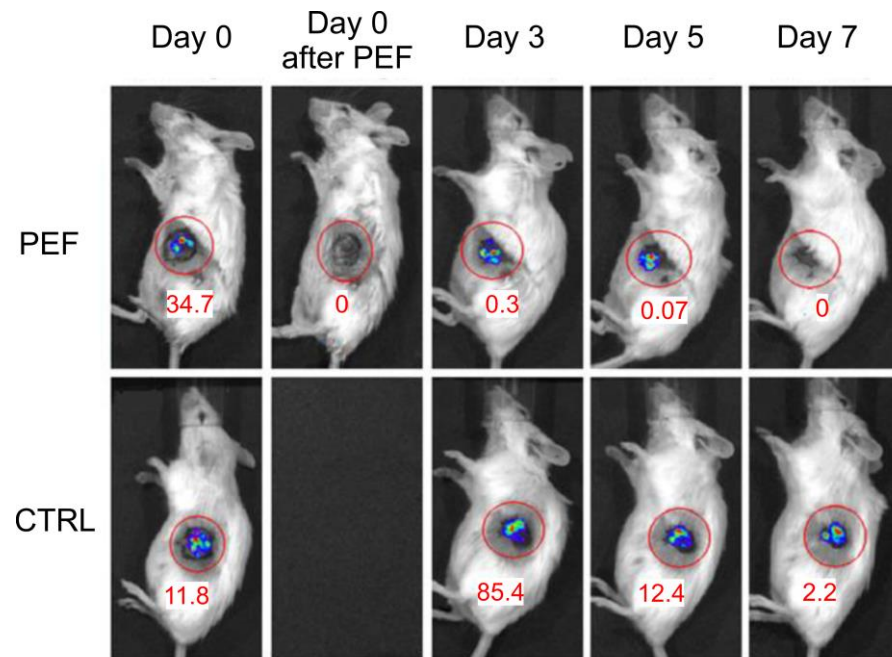


Figure 5. The mice with only the AA (1%) treatment (CTRL) and the mice treated with PEF (3 kV voltage is applied between 1.2 mm gap electrodes) + 1% AA treatment. Red circle indicates region of interest (ROI) where the luminescence signal was quantified. The number indicates the intensity of luminescence in the ROI.

It can be seen that AA with a concentration as low as 1% does not result in a successful treatment. The luminescence signal increased almost eight-fold on day 3, indicating an increased number of bacterial cells, which is proportional to the luminescence.

At the same time, PEF + AA treatment results in the effective killing of bacteria. Shortly after the treatment, the luminescence signal was beyond the detection limits of our infrastructure. On day 3, in some experimental mice, a weak signal could be detected; however, in general, it was lower when compared to the AA-only treatment.

The quantified results with both nanosecond protocols are shown in Figure 6. It can be seen that there is a positive response to both treatments; however, the 3 kV treatment is more effective.

The standard deviation is also significantly lower when the 3 kV protocol is employed, which results in a statistically significant ($p < 0.001$) decrease in the luminescence signal (i.e., bacterial viability) when compared to PEF-untreated mice. It should be also noted that the variation in response may partly be dependent on the human factor and the accuracy of electrode repositioning. A total of 14 ± 5 repositions of the tweezer electrodes was required to cover the whole treatment area.

In order to determine the immune response to bacterial infection, IgM and IgG (IgG1, IgG2a, IgG2b, IgG3) antibodies against *P. aeruginosa* surface and intracellular antigens were evaluated. Based on the results presented in Figure 6, the study was limited to the 3 kV protocol. The data are summarized in Figure 7.

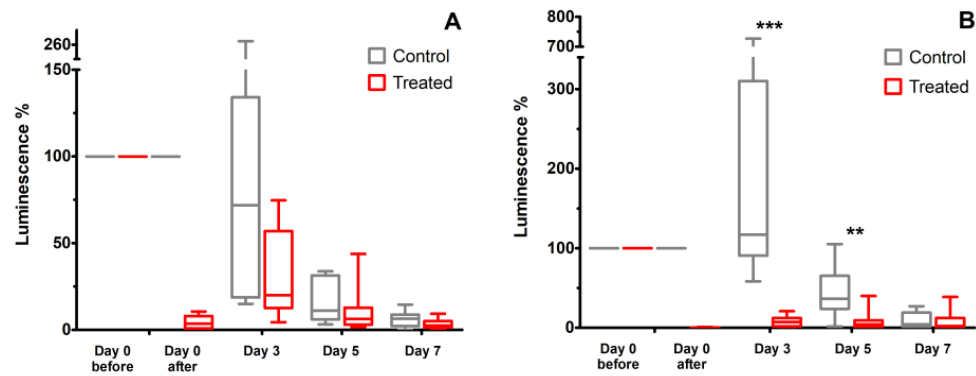


Figure 6. The luminescence of the ROI after the treatment using 1.8 kV protocol (A) and 3 kV protocol (B). All the data were normalized to the CTRL group. Asterisks: ** $p \leq 0.01$; *** $p \leq 0.001$.

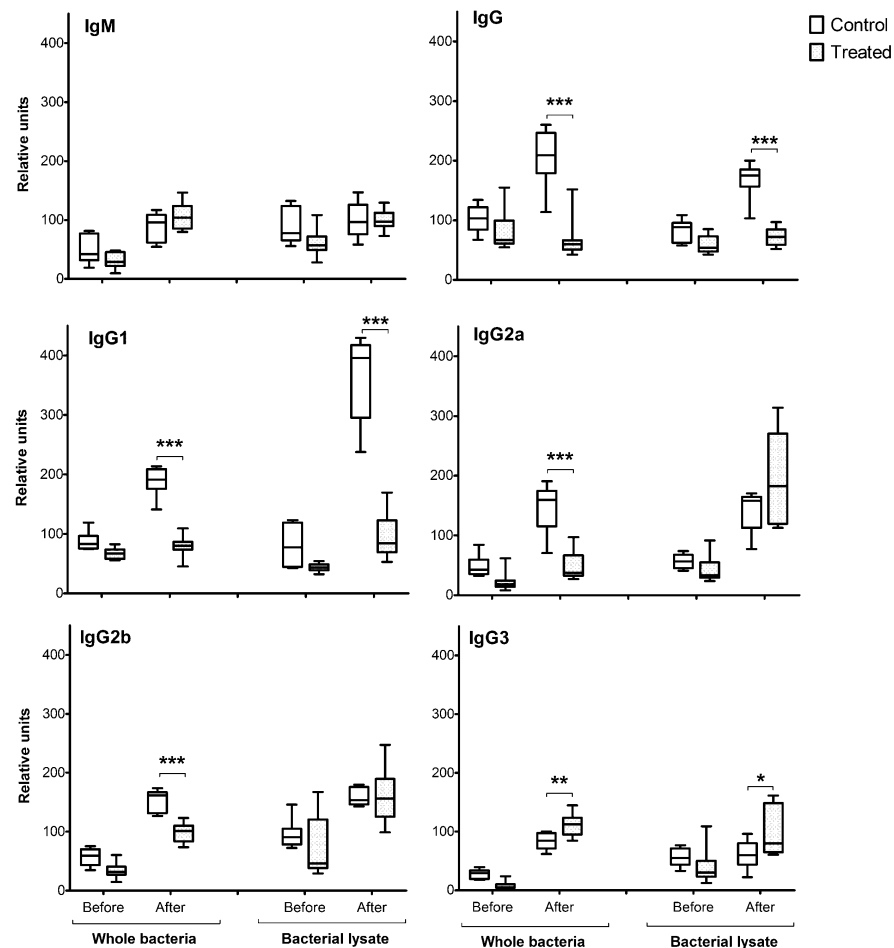


Figure 7. Relative units of immunoglobulin G isotypes IgG1, IgG2a, IgG2b and IgG3 antibodies in blood sera of the control (PEF untreated) and PEF-treated (3 kV, 1.2 mm gap) mice. Whole bacteria graphs represent the amounts of antibodies produced against surface antigens of *P. aeruginosa* and bacterial lysate against intracellular antigens. The white columns represent the antibody levels detected in the blood sera of control mice, and the gray columns represent the PEF-treated ones. Asterisk (*) corresponds to statistically significant differences (* $p \leq 0.05$; ** $p \leq 0.01$; *** $p \leq 0.001$).

As can be seen, the relative units of surface and intracellular IgM Ab in control and PEF-treated mice’s blood serum had no statistically significant differences before and after the PEF treatment. However, significant differences were observed when evaluating IgG class Ab, regardless of whether they formed against surface or intracellular bacterial Ag.

The relative units of surface IgG and IgG1 antibodies were significantly lower in the murine serum of PEF-treated mice, compared to the bacterial-infection-bearing mice (treated with AA only). At the same time, no significant differences between bacterial-infection-bearing mice (treated with AA only) and PEF-treated mice groups were observed when evaluating IgG2a and IgG2b antibodies against intracellular bacterial antigens. Moreover, IgG3 antibodies against surface and intracellular bacterial antigens were significantly increased in PEF-treated mice's blood sera, compared to bacterial-infection-bearing mice (treated with AA only).

4. Discussion

In this work, we have developed an in vivo superficial bacterial infection model using clinically relevant bacteria (*P. aeruginosa*) and showed the application potential of nanosecond electroporation for the killing of bacteria. We have improved the recent concept presented by Wu et al. [28] and provided experimental data on bacterial growth dynamics throughout the week, which was not possible with a previous model [5].

The proposed nanosecond methodology does not require us to create a skin fold, which, in many clinical cases, is impossible due to the complex morphology of the wound and surrounding tissue. We have shown that the tweezer electrodes can induce a sufficient electric field for the inactivation of bacteria when combined with low concentrations of acetic acid. This methodology is a hybrid of the tissue ablation [42,43] and electrochemotherapy [44] methods, which are used in the cancer treatment context. In our work, based on FEM simulation, we conclude that the small gap (1.2 mm) between the electrodes ensures the superficial permeabilization of cells without affecting the deeper tissues. The inhomogeneity of the electric field should be compensated by a higher field intensity (in our case, 3 kV at 1.2 mm gap) or unsatisfactory bacterial killing efficiency will be triggered (Figure 6A).

The input energy of the proposed PEF protocols is lower compared to available research on this topic [19,28]. Minimizing the energy is advantageous since a non-thermal procedure can be ensured, while the application of bursts of microsecond pulses with a high-intensity electric field results in significant Joule heating [45]. In our work, the temperature rise based on FEM is >20 °C, which indicates the need to reduce the input energy even further to ensure a non-thermal procedure. Additionally, moving towards the shorter pulse duration range reduces muscle contractions [46] and potentially pain [47].

We have also used low-concentration acetic acid (1%), showing a synergistic effect with electroporation (i.e., electrochemotherapy), which supports our preliminary in vitro [29] and in vivo data [5]. It should be noted that we have modeled a superficial infection. In essence, the skin was mechanically irritated for the bacteria to colonize. However, in the case of chronic wounds, the methodology should be further optimized to account for the possible non-homogeneity of the PEF spatial distribution due to the complex morphology of the treatment area. Additionally, the method can be supplemented with various patching and wound dressing techniques [48,49].

In terms of pulsing, the methodology can be also improved. We have used a 3 kV charging voltage (limitation of our infrastructure) to induce up to a 25 kV/cm electric field, which is sufficient to kill the bacteria with acetic acid; however, the application of a higher-intensity electric field (but a shorter pulse duration and smaller number of pulses) should potentially even further improve the input energy management [50]. The PEF alone, without any chemotherapeutic agents, can be also used; however, the intensity of PEF should be increased to ensure irreversible electroporation. As a matter for future work, the application of high-frequency bipolar or MHz-range unipolar pulses should be considered [51–53]. High-frequency bipolar pulses enable the mitigation of the impedance changes and a more uniform treatment [54], while compressing the pulses to a MHz burst significantly lowers the electroporation threshold [55,56]. However, in this case, the effects of Joule heating should be considered and a trade-off between the input energy and the resultant Joule heating should be sought.

In this work, *P. aeruginosa* was used as a cell model. Gram-negative bacteria are one of the most resistant types of microorganisms to PEF due to the specific structure of the cell wall [57]. It implies that the proposed method is even more compatible with superficial infections by fungi, yeast or Gram-positive bacteria due to their higher susceptibility to PEF [58–60]. However, further *in vivo* research is required to confirm this hypothesis.

In terms of the immune response, we have shown that the PEF + AA treatment triggers significant changes in the levels of surface IgG, IgG1 and IgG2 antibodies. After the treatment, the response is comparable to the groups of mice without the infection (Figure 7, control group “before”). IgG1 is one of the most functional subclasses of antibodies, due to its superior affinity to FcγR, while IgG2 also plays an important role in targeting polysaccharides and is commonly induced during bacterial infections [61,62]. Our data indicate that the reduction in both IgG1 and IgG2 is associated with reduced bacterial infection and an anti-inflammatory effect following the treatment, which shows no contrast with data presented by Wu et al. [28].

As a limitation of our study, we could highlight the fact that it was a proof-of-concept work, where we aimed to characterize the synergistic PEF + AA treatment compared to AA-only treatment based on an available bioethical protocol. However, as a matter for future work, it would be useful to characterize the effects of PEF alone and AA alone, and to determine the optimal conditions and concentrations for PEF + AA treatment. Moreover, the development of an *in vivo* wound model with the possibility to induce biofilms would significantly improve the accuracy of the model and the treatment planning.

To conclude, nanosecond PEF + AA treatment shows promising results for the treatment of superficial infections, while it requires further optimization in terms of pulse parameters and the optimal concentration of AA. Acetic acid is routinely used in burn wound contexts since it does not contribute to the development of drug resistance in bacteria, while electroporation has been applied in clinics for decades to treat superficial and deep-seated cancer. Therefore, the transition of the proposed methodology to a clinical context is merely a matter of time due to the already established safety and treatment planning measures. The available clinical electroporators can be employed.

Author Contributions: Conceptualization, V.N., I.G. and A.Z.; methodology, V.N. and I.G.; investigation, E.P., E.R. and V.M.-P.; resources, J.N. and I.G.; writing—original draft preparation, V.N. and E.R.; writing—review and editing, E.P., E.R., V.M.-P., A.Z. and J.N.; visualization, V.N., E.P. and V.M.-P.; supervision, V.N. and I.G. All authors have read and agreed to the published version of the manuscript.

Funding: This research was funded by Research Council of Lithuania grant number LAT-02/2016.

Institutional Review Board Statement: The protocol was approved by the State Food and Veterinary Service (License Nr. G2-48).

Informed Consent Statement: Not applicable.

Data Availability Statement: Data are available from the corresponding author V.N. on request.

Conflicts of Interest: The authors declare no conflict of interest.

References

1. Moradpoor, H.; Mohammadi, H.; Safaei, M.; Mozaffari, H.R.; Sharifi, R.; Gorji, P.; Sulong, A.B.; Muhamad, N.; Ebadi, M. Recent Advances on Bacterial Cellulose-Based Wound Management: Promises and Challenges. *Int. J. Polym. Sci.* **2022**, *2022*, 1214734. [[CrossRef](#)]
2. Jin, L.; Cheng, H.; Xie, X.; Chen, X.; Tian, G.; Zhu, Z.; Wang, S.; Xin, H.; Wang, X. Dual-Effective Chronic Wounds Management System through a Monoglyceride Binary Blend Matrix Based Thermal-Responsive Phase-Transition Substrate. *Adv. Healthc. Mater.* **2021**, *10*, e2001966. [[CrossRef](#)] [[PubMed](#)]
3. Hossain, M.L.; Rahman, M.A.; Siddika, A.; Adnan, M.H.; Rahman, H.; Diba, F.; Hasan, M.Z.; Asaduzzaman, S.M. Burn and Wound Healing Using Radiation Sterilized Human Amniotic Membrane and Centella asiatica Derived Gel: A Review. *Regen. Eng. Transl. Med.* **2020**, *6*, 347–357. [[CrossRef](#)]
4. Gallaher, J.R.; Banda, W.; Lachiewicz, A.M.; Krysiak, R.; Purcell, L.N.; Charles, A.G. Predictors of multi-drug resistance in burn wound colonization following burn injury in a resource-limited setting. *Burns* **2021**, *47*, 1308–1313. [[CrossRef](#)] [[PubMed](#)]

5. Novickij, V.; Zinkevičienė, A.; Perminaitė, E.; Česna, R.; Lastauskienė, E.; Paškevičius, A.; Švedienė, J.; Markovskaja, S.; Novickij, J.; Girkontaitė, I. Non-invasive nanosecond electroporation for biocontrol of surface infections: An in vivo study. *Sci. Rep.* **2018**, *8*, 14516. [[CrossRef](#)] [[PubMed](#)]
6. Willyard, C. Drug-resistant bacteria ranked. *Nature* **2017**, *543*, 15. [[CrossRef](#)]
7. Javanmardi, F.; Emami, A.; Pirbonyeh, N.; Keshavarzi, A.; Rajaei, M. A systematic review and meta-analysis on Exo-toxins prevalence in hospital acquired *Pseudomonas aeruginosa* isolates. *Infect. Genet. Evol.* **2019**, *75*, 104037. [[CrossRef](#)]
8. Hasannejad-Bibalan, M.; Jafari, A.; Sabati, H.; Goswami, R.; Jafaryparvar, Z.; Sedaghat, F.; Sedigh Ebrahim-Saraie, H. Risk of type III secretion systems in burn patients with *Pseudomonas aeruginosa* wound infection: A systematic review and meta-analysis. *Burns* **2021**, *47*, 538–544. [[CrossRef](#)]
9. Hopman, J.; Meijer, C.; Kenters, N.; Coolen, J.P.M.; Ghamati, M.R.; Mehtar, S.; Van Crevel, R.; Morshuis, W.J.; Verhagen, A.F.T.M.; Van Den Heuvel, M.M.; et al. Risk Assessment after a Severe Hospital-Acquired Infection Associated with Carbapenemase-Producing *Pseudomonas aeruginosa*. *JAMA Netw. Open* **2019**, *2*, e187665. [[CrossRef](#)]
10. Tümmler, B. Emerging therapies against infections with *Pseudomonas aeruginosa*. *F1000Research* **2019**, *8*, 1371. [[CrossRef](#)]
11. Azzopardi, E.A.; Azzopardi, E.; Camilleri, L.; Villapalos, J.; Boyce, D.E.; Dziejewski, P.; Dickson, W.A.; Whitaker, I.S. Gram negative wound infection in hospitalised adult burn patients-systematic review and metanalysis-. *PLoS ONE* **2014**, *9*, e95042. [[CrossRef](#)] [[PubMed](#)]
12. Jinks, T.; Lee, N.; Sharland, M.; Rex, J.; Gertler, N.; Diver, M.; Jones, I.; Jones, K.; Mathewson, S.; Chiara, F.; et al. A time for action: Antimicrobial resistance needs global response. *Bull. World Health Organ.* **2016**, *94*, 558–558A. [[CrossRef](#)] [[PubMed](#)]
13. Sloss, J.M.; Cumberland, N.; Milner, S.M. Acetic acid used for the elimination of *Pseudomonas aeruginosa* from burn and soft tissue wounds. *J. R. Army Med. Corps* **1993**, *139*, 49–51. [[CrossRef](#)]
14. Halstead, F.D.; Rauf, M.; Moiemien, N.S.; Bamford, A.; Wearn, C.M.; Fraise, A.P.; Lund, P.A.; Oppenheim, B.A.; Webber, M.A. The antibacterial activity of acetic acid against biofilm-producing pathogens of relevance to burns patients. *PLoS ONE* **2015**, *10*, e0136190. [[CrossRef](#)]
15. Nagoba, B.S.; Selkar, S.P.; Wadher, B.J.; Gandhi, R.C. Acetic acid treatment of pseudomonal wound infections—A review. *J. Infect. Public Health* **2013**, *6*, 410–415. [[CrossRef](#)]
16. Ning, X.; He, G.; Zeng, W.; Xia, Y. The photosensitizer-based therapies enhance the repairing of skin wounds. *Front. Med.* **2022**, *9*, 915548. [[CrossRef](#)]
17. Dubey, S.K.; Parab, S.; Alexander, A.; Agrawal, M.; Achalla, V.P.K.; Pal, U.N.; Pandey, M.M.; Kesharwani, P. Cold atmospheric plasma therapy in wound healing. *Process. Biochem.* **2022**, *112*, 112–123. [[CrossRef](#)]
18. Ferguson, M.; Byrnes, C.; Sun, L.; Marti, G.; Bonde, P.; Duncan, M.; Harmon, J.W. Wound healing enhancement: Electroporation to address a classic problem of military medicine. *World J. Surg.* **2005**, *29*, 55–59. [[CrossRef](#)] [[PubMed](#)]
19. Golberg, A.; Broelsch, G.F.; Vecchio, D.; Khan, S.; Hamblin, M.R.; Austen, W.G.; Sheridan, R.L.; Yarmush, M.L. Pulsed electric fields for burn wound disinfection in a murine model. *J. Burn Care Res.* **2016**, *36*, 7–13. [[CrossRef](#)]
20. Khan, S.I.; Blumrosen, G.; Vecchio, D.; Golberg, A.; McCormack, M.C.; Yarmush, M.L.; Hamblin, M.R.; Austen, W.G. Eradication of multidrug-resistant *Pseudomonas* biofilm with pulsed electric fields. *Biotechnol. Bioeng.* **2016**, *113*, 643–650. [[CrossRef](#)]
21. Saulis, G. Electroporation of cell membranes: The fundamental effects of pulsed electric fields in food processing. *Food Eng. Rev.* **2010**, *2*, 52–73. [[CrossRef](#)]
22. Kotnik, T.; Kramar, P.; Pucihar, G.; Miklavčič, D.; Tarek, M. Cell membrane electroporation—Part 1: The phenomenon. *IEEE Electr. Insul. Mag.* **2012**, *28*, 14–23. [[CrossRef](#)]
23. Of, J.; Biology, M.; Mahni, S.; Universit, K.; Universit, E.V. Electroporation in Food Processing and Biorefinery Electroporation in Food Processing and Biorefinery. *J. Membr. Biol.* **2014**, *247*, 1279–1304. [[CrossRef](#)]
24. Novickij, V.; Švedienė, J.; Paškevičius, A.; Markovskaja, S.; Lastauskienė, E.; Zinkevičienė, A.; Girkontaitė, I.; Novickij, J. Induction of Different Sensitization Patterns of MRSA to Antibiotics Using Electroporation. *Molecules* **2018**, *23*, 1799. [[CrossRef](#)]
25. Novickij, V.; Švedienė, J.; Paškevičius, A.; Markovskaja, S.; Girkontaitė, I.; Zinkevičienė, A.; Lastauskienė, E.; Novickij, J.; Svediene, J.; Markovskaja, S.; et al. Pulsed electric field-assisted sensitization of multidrug-resistant *Candida albicans* to antifungal drugs. *Future Microbiol.* **2018**, *13*, 535–546. [[CrossRef](#)] [[PubMed](#)]
26. Ravensdale, J.; Wong, Z.; O'Brien, F.; Gregg, K. Efficacy of antibacterial peptides against peptide-resistant mrsa is restored by permeabilization of bacteria membranes. *Front. Microbiol.* **2016**, *7*, 1745. [[CrossRef](#)]
27. Lovšin, Ž.; Klančnik, A.; Kotnik, T. Electroporation as an Efficacy Potentiator for Antibiotics with Different Target Sites. *Front. Microbiol.* **2021**, *12*, 722232. [[CrossRef](#)] [[PubMed](#)]
28. Wu, M.; Rubin, A.E.; Dai, T.; Schloss, R.; Usta, O.B.; Golberg, A.; Yarmush, M. High-Voltage, Pulsed Electric Fields Eliminate *Pseudomonas aeruginosa* Stable Infection in a Mouse Burn Model. *Adv. Wound Care* **2021**, *10*, 477–489. [[CrossRef](#)]
29. Novickij, V.; Lastauskienė, E.; Staigvila, G.; Girkontaitė, I.; Zinkevičienė, A.; Švedienė, J.; Paškevičius, A.; Markovskaja, S.; Novickij, J. Low concentrations of acetic and formic acids enhance the inactivation of *Staphylococcus aureus* and *Pseudomonas aeruginosa* with pulsed electric fields. *BMC Microbiol.* **2019**, *19*, 73. [[CrossRef](#)]
30. Chang, R.Y.K.; Das, T.; Manos, J.; Kutter, E.; Morales, S.; Chan, H.K. Bacteriophage PEV20 and Ciprofloxacin Combination Treatment Enhances Removal of *Pseudomonas aeruginosa* Biofilm Isolated from Cystic Fibrosis and Wound Patients. *AAPS J.* **2019**, *21*, 49. [[CrossRef](#)]

31. Novickij, V.; Grainys, A.; Butkus, P.; Tolvaišienė, S.; Švedienė, J.; Paškevičius, A.; Novickij, J. High-frequency submicrosecond electroporator. *Biotechnol. Biotechnol. Equip.* **2016**, *30*, 607–613. [[CrossRef](#)]
32. Campana, L.G.; Edhemovic, I.; Soden, D.; Perrone, A.M.; Scarpa, M.; Campanacci, L.; Cemazar, M.; Valpione, S.; Miklavčič, D.; Mocellin, S.; et al. Electrochemotherapy—Emerging applications technical advances, new indications, combined approaches, and multi-institutional collaboration. *Eur. J. Surg. Oncol.* **2019**, *45*, 92–102. [[CrossRef](#)] [[PubMed](#)]
33. Hughes, A.J.; Tawfik, S.S.; Baruah, K.P.; O’Toole, E.A.; O’Shaughnessy, R.F.L. Tape strips in dermatology research. *Br. J. Dermatol.* **2021**, *185*, 26–35. [[CrossRef](#)]
34. Pavšelj, N.; Préat, V.; Miklavčič, D. A numerical model of skin electroporabilization based on in vivo experiments. *Ann. Biomed. Eng.* **2007**, *35*, 2138–2144. [[CrossRef](#)] [[PubMed](#)]
35. Corovic, S.; Lackovic, I.; Sustaric, P.; Sustar, T.; Rodic, T.; Miklavcic, D. Modeling of electric field distribution in tissues during electroporation. *Biomed. Eng. Online* **2013**, *12*, 16. [[CrossRef](#)]
36. Pavšelj, N.; Miklavčič, D. Resistive heating and electroporabilization of skin tissue during in vivo electroporation: A coupled nonlinear finite element model. *Int. J. Heat Mass Transf.* **2011**, *54*, 2294–2302. [[CrossRef](#)]
37. Guo, Y.; Dreier, J.R.; Cao, J.; Du, H.; Granter, S.R.; Kwiatkowski, D.J. Analysis of a mouse skin model of tuberous sclerosis complex. *PLoS ONE* **2016**, *11*, e0167384. [[CrossRef](#)] [[PubMed](#)]
38. Yu, K.; Shao, Q.; Ashkenazi, S.; Bischof, J.C.; He, B. In Vivo Electrical Conductivity Contrast Imaging in a Mouse Model of Cancer Using High-Frequency Magnetoacoustic Tomography With Magnetic Induction (hfMAT-MI). *IEEE Trans. Med. Imaging* **2016**, *35*, 2301–2311. [[CrossRef](#)]
39. Callister, W. *Materials Science and Engineering: An Introduction, Jr.—7th ed. p. cm., TA403.C23 2007*; John Wiley & Sons: Hoboken, NJ, USA, 2007; ISBN 9780471736967.
40. Kaewthong, P.; Wattanachant, S. Optimizing the electrical conductivity of marinade solution for water-holding capacity of broiler breast meat. *Poult. Sci.* **2018**, *97*, 701–708. [[CrossRef](#)]
41. Curnow, O.J.; MacFarlane, D.R.; Walst, K.J. Fluoride ionic liquids in salts of ethylmethylimidazolium and substituted cyclopropenium cation families. *Front. Chem.* **2018**, *6*, 603. [[CrossRef](#)]
42. Fesmire, C.C.; Petrella, R.A.; Kaufman, J.D.; Topasna, N.; Sano, M.B. Irreversible electroporation is a thermally mediated ablation modality for pulses on the order of one microsecond. *Bioelectrochemistry* **2020**, *135*, 107544. [[CrossRef](#)] [[PubMed](#)]
43. Ruarus, A.H.; Barabasch, A.; Catalano, O.; Leen, E.; Narayanan, G.; Nilsson, A.; Padia, S.A.; Wiggermann, P.; Scheffer, H.J.; Meijerink, M.R. Irreversible Electroporation for Hepatic Tumors: Protocol Standardization Using the Modified Delphi Technique. *J. Vasc. Interv. Radiol.* **2020**, *31*, 1765–1771.e15. [[CrossRef](#)]
44. Cemazar, M.; Sersa, G. Recent Advances in Electrochemotherapy. *Bioelectricity* **2019**, *1*, 204–213. [[CrossRef](#)] [[PubMed](#)]
45. Ruarus, A.H.; Vroomen, L.G.P.H.; Puijk, R.S.; Scheffer, H.J.; Faes, T.J.C.; Meijerink, M.R. Conductivity Rise During Irreversible Electroporation: True Permeabilization or Heat? *Cardiovasc. Intervent. Radiol.* **2018**, *41*, 1257–1266. [[CrossRef](#)] [[PubMed](#)]
46. Mi, Y.; Xu, J.; Tang, X.; Bian, C.; Liu, H.; Yang, Q.; Tang, J. Scaling relationship of in vivo muscle contraction strength of rabbits exposed to high-frequency nanosecond pulse bursts. *Technol. Cancer Res. Treat.* **2018**, *17*. [[CrossRef](#)]
47. Fusco, R.; Di Bernardo, E.; D’Alessio, V.; Salati, S.; Cadossi, M. Reduction of muscle contraction and pain in electroporation-based treatments: An overview. *World J. Clin. Oncol.* **2021**, *12*, 367–381. [[CrossRef](#)]
48. Wang, Y.; Guo, M.; He, B.; Gao, B. Intelligent Patches for Wound Management: In Situ Sensing and Treatment. *Anal. Chem.* **2021**, *93*, 4687–4696. [[CrossRef](#)]
49. Khona, D.K.; Roy, S.; Ghatak, S.; Huang, K.; Jagdale, G.; Baker, L.A.; Sen, C.K. Ketoconazole resistant *Candida albicans* is sensitive to a wireless electrochemical wound care dressing. *Bioelectrochemistry* **2021**, *142*, 107921. [[CrossRef](#)]
50. Schoenbach, K.; Joshi, R.; Beebe, S.; Baum, C. A scaling law for membrane permeabilization with nanopulses. *IEEE Trans. Dielectr. Electr. Insul.* **2009**, *16*, 1224–1235. [[CrossRef](#)]
51. Vižintin, A.; Marković, S.; Ščančar, J.; Miklavčič, D. Electroporation with nanosecond pulses and bleomycin or cisplatin results in efficient cell kill and low metal release from electrodes. *Bioelectrochemistry* **2021**, *140*, 107798. [[CrossRef](#)]
52. Novickij, V.; Ruzgys, P.; Grainys, A.; Šatkauskas, S. High frequency electroporation efficiency is under control of membrane capacitive charging and voltage potential relaxation. *Bioelectrochemistry* **2018**, *119*, 92–97. [[CrossRef](#)] [[PubMed](#)]
53. Semenov, I.; Casciola, M.; Ibey, B.L.; Xiao, S.; Pakhomov, A.G. Electroporabilization of cells by closely spaced paired nanosecond-range pulses. *Bioelectrochemistry* **2018**, *121*, 135–141. [[CrossRef](#)] [[PubMed](#)]
54. Bhonsle, S.P.; Arena, C.B.; Sweeney, D.C.; Davalos, R.V. Mitigation of impedance changes due to electroporation therapy using bursts of high-frequency bipolar pulses. *Biomed. Eng. Online* **2015**, *14* (Suppl. S3), S3. [[CrossRef](#)] [[PubMed](#)]
55. Radzevičiūtė, E.; Malyško-Ptašinskė, V.; Kulbacka, J.; Rembialkowska, N.; Novickij, J.; Girkontaitė, I.; Novickij, V. Nanosecond electrochemotherapy using bleomycin or doxorubicin: Influence of pulse amplitude, duration and burst frequency. *Bioelectrochemistry* **2022**, *148*, 108251. [[CrossRef](#)]
56. Pakhomov, A.G.A.G.; Xiao, S.; Novickij, V.; Casciola, M.; Semenov, I.; Mangalanathan, U.; Kim, V.; Zemlin, C.; Sozer, E.; Muratori, C.; et al. Excitation and electroporation by MHz bursts of nanosecond stimuli. *Biochem. Biophys. Res. Commun.* **2019**, *518*, 759–764. [[CrossRef](#)] [[PubMed](#)]
57. Pillet, F.; Formosa-Dague, C.; Baaziz, H.; Dague, E.; Rols, M.-P. Cell wall as a target for bacteria inactivation by pulsed electric fields. *Sci. Rep.* **2016**, *6*, 19778. [[CrossRef](#)]

58. Garner, A.L. Pulsed electric field inactivation of microorganisms: From fundamental biophysics to synergistic treatments. *Appl. Microbiol. Biotechnol.* **2019**, *103*, 7917–7929. [[CrossRef](#)]
59. Simonis, P.; Kersulis, S.; Stankevich, V.; Kaset, V.; Lastauskiene, E.; Stirke, A. Caspase dependent apoptosis induced in yeast cells by nanosecond pulsed electric fields. *Bioelectrochemistry* **2017**, *115*, 19–25. [[CrossRef](#)]
60. Novickij, V.; Švedienė, J.; Paškevičius, A.; Novickij, J.; Svediene, J.; Paskevicius, A.; Novickij, J. In vitro evaluation of nanosecond electroporation against *Trichophyton rubrum* with or without antifungal drugs and terpenes. *Mycoscience* **2017**, *58*, 261–266. [[CrossRef](#)]
61. Damelang, T.; Rogerson, S.J.; Kent, S.J.; Chung, A.W. Role of IgG3 in Infectious Diseases. *Trends Immunol.* **2019**, *40*, 197–211. [[CrossRef](#)]
62. Michaelsen, T.E.; Kolberg, J.; Aase, A.; Herstad, T.K.; Høiby, E.A. The four mouse IgG isotypes differ extensively in bactericidal and opsonophagocytic activity when reacting with the P1.16 epitope on the outer membrane PorA protein of *Neisseria meningitidis*. *Scand. J. Immunol.* **2004**, *59*, 34–39. [[CrossRef](#)] [[PubMed](#)]

Disclaimer/Publisher’s Note: The statements, opinions and data contained in all publications are solely those of the individual author(s) and contributor(s) and not of MDPI and/or the editor(s). MDPI and/or the editor(s) disclaim responsibility for any injury to people or property resulting from any ideas, methods, instructions or products referred to in the content.